Template Synthesis of Two-Dimensional Network of Cross-Linked Acrylate Polymer in a Cast Multibilayer Film

Sumitoshi Asakuma, Hideo Okada, and Toyoki Kunitake*,†

Contribution from the Molecular Architecture Project, JRDC, Kurume Research Park, Kurume 830, Japan. *Received July 23, 1990*

Abstract: Cast multibilayer films were prepared from aqueous dispersions of a double-chain ammonium amphiphile and a bisacrylate monomer. X-ray diffraction and the structure simulation by electron density matching showed that the lamellar molecular packing in a single-component cast film was modified upon addition of the monomer so that the monomer can be incorporated uniformly into the void near the bilayer surface. The depth profile of the element distribution as determined by X-ray photoelectron spectroscopy was consistent with this supposition. UV irradiation of the composite cast film produced an extensively cross-linked polymer without detectable structural changes of the template film. Extraction of the amphiphile component with methanol left behind a multilayered film of the two-dimensional polymer network. Solvent swelling and some mechanical properties reflected the characteristic structural anisotropy. It is concluded that cast multibilayer films provide superior templates for preparation of two-dimensional network structures of molecular thickness.

Introduction

Synthetic bilayer membranes[1-4] are highly organized molecular aggregates, and their characteristic organizations are maintained not only in aqueous dispersions such as vesicles and lamellae but also in their cast films. The regular multibilayer structure of these cast films has been used as a matrix for specific binding of cyanine dyes,[5] anisotropic orientation of metal chelates,[6] and topotactic polymerization of the diacetylene unit.[7] The interbilayer space of the cast film also acts as an extended two-dimensional matrix similar to the interlayer spaces of montmorillonite and graphite.

Extended two-dimensionality of a binding site can be probed conveniently by formation and isolation of polymeric networks. The past examples of matrix-controlled synthesis of the two-dimensional network include cross-linking of poly(ethylenimine) adsorbed on alumina particles with glutaraldehyde,[8] polymerization of vinyl monomers[9-11] and formation of a polyion complex[12] at the air-water interface, polymerization at an oil-water interface,[13] polymerization of styrene within adsorbed monolayers,[14] polymerization on the surface of aqueous bilayer dispersions,[15-17] and formation of graphite by pyrolysis of poly(acrylonitrile) in the interlayer of montmorillonite.[18,19]

We have shown briefly that cast films of synthetic bilayer membranes provide matrices for preparation of two-dimensional molecular networks (both organic[20] and inorganic[21,22]). The present paper describes a detailed examination of the molecular organization of cast films of double-chain ammonium amphiphile **1** and its composite with a bisacrylate monomer **2** or polymer. The high regularity observed for the composite film is a prerequisite of a template for the synthesis of a two-dimensional polymer network. It is established that cast films of synthetic bilayer membranes are superior templates for preparation of two-dimensional materials.

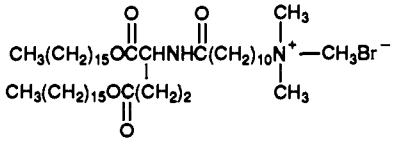

amphiphile **1**

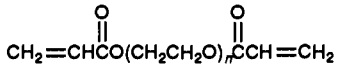

n ≈ 14
monomer **2**

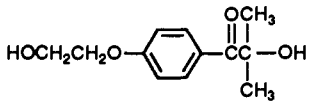

initiator **3**

Experimental Section

Materials. Ammonium amphiphile **1** was prepared as follows. L-Glutamic acid (10 g, 0.068 mol), 14 g (0.074 mol) of *p*-toluenesulfonic acid, and 38 g (0.16 mol) of hexadecanol were dissolved in toluene, and water was removed as an azeotropic mixture with a Dean-Stark trap. The reaction was continued until the stoichiometric amount of water was recovered. Toluene was removed, and the precipitates were recrystallized from acetone: colorless powder; yield 81%. The product diester was identified by IR and NMR spectra. A chloroform solution of 3.0 g (3.8 × 10^{-3} mol) of the diester and 0.81 g (8.0 × 10^{-3} mol) of triethylamine was added dropwise to a chloroform solution of 11-bromoundecanoyl chloride (1.1 g, 4.0 × 10^{-3} mol), and the mixture was stirred for 24 h at room temperature. Chloroform was removed, and the residue was recrystallized from hexane: colorless powder; yield 64%. The amide product was confirmed by IR and NMR spectra and quaternized with trimethylamine in THF at room temperature for 4 days. After removal of excess trimethylamine and THF, the residue was recrystallized from

† Permanent address: Department of Organic Synthesis, Faculty of Engineering, Kyushu University, Fukuoka 812, Japan.

(1) Fendler, J. H. *Membrane Mimetic Chemistry*; Wiley-Interscience: New York, 1982; Chapter 6.
(2) Ringsdorf, H.; Schlarb, B.; Venzmer, J. *Angew. Chem., Int. Ed. Engl.* **1988**, *27*, 113-158.
(3) Fuhrhop, J.-J.; Mathieu, J. *Angew. Chem., Int. Ed. Engl.* **1984**, *23*, 100-113.
(4) Kunitake, T. *Angew. Chem., Int. Ed. Engl.*, in press.
(5) Nakashima, N.; Ando, R.; Kunitake, T. *Chem. Lett.* **1983**, 1577-1580.
(6) Ishikawa, Y.; Kunitake, T. *J. Am. Chem. Soc.* **1986**, *108*, 8300-8302.
(7) Kuo, T.; O'Brien, D. F. *J. Am. Chem. Soc.* **1988**, *110*, 7571-7572.
(8) Meyers, W. E.; Royer, G. P. *J. Am. Chem. Soc.* **1977**, *99*, 6141-6142.
(9) Dubault, A.; Casagrande, C.; Veyssie, M. *J. Phys. Chem.* **1975**, *79*, 2254-2259.
(10) Barraud, A.; Rosilio, C.; Ruaudel-Teixier, A. *Polym. Prepr. (Am. Chem. Soc., Div. Polym. Chem.)* **1978**, *19*, 179-182.
(11) Laschewsky, A.; Ringsdorf, H.; Schmidt, G. *Thin Solid Films* **1985**, *134*, 153-172.
(12) Kunitake, T.; Higashi, N.; Kunitake, M.; Fukushige, Y. *Macromolecules* **1989**, *22*, 485-487.
(13) Rehage, H.; Schnabel, E.; Veyssie, M. *Makromol. Chem.* **1988**, *189*, 2395-2408.
(14) Wu, J.; Harwell, J. H.; O'Rear, E. A. *Langmuir* **1987**, *3*, 531-537.
(15) Ringsdorf, H.; Schlarb, B. *Makromol. Chem.* **1988**, *189*, 299-315.
(16) Ringsdorf, H.; Tyminski, P. N.; O'Brien, D. F. *Macromolecules* **1988**, *21*, 671-677.
(17) Kunitake, T.; Nakashima, N.; Kunitake, M. *Macromolecules* **1989**, *22*, 3544-3550.
(18) Kyotani, T.; Sonobe, N.; Tomita, A. *Nature (London)* **1988**, *331*, 331-333.
(19) Sonobe, N.; Kyotani, T.; Tomita, A. *Carbon* **1988**, *26*, 573-578.
(20) Asakuma, S.; Kunitake, T. *Chem. Lett.* **1989**, 2059-2062.
(21) Sakata, K.; Kunitake, T. *Chem. Lett.* **1989**, 2159-2162.
(22) Sakata, K.; Kunitake, T. *J. Chem. Soc., Chem. Commun.* **1990**, 504-505.

0002-7863/91/1513-1749$02.50/0

ethyl acetate: colorless powder; yield 68%; mp 66→141 °C (the arrow indicates the liquid–crystalline region); IR (KBr, cm^{-1}) 3314 (ν_{N-H}, amide), 2922 (ν_{C-H}, methylene), 2852 (ν_{C-H}, methylene), 1729 ($\nu_{C=O}$, ester), 1643 ($\nu_{C=O}$, amide). Anal. Calcd for $C_{51}H_{101}O_5N_2Br \cdot H_2O$: C, 66.56; H, 11.28; N, 3.04. Found: C, 66.44; H, 11.24; N, 2.96. The presence of hydrated water was supported by a broad IR peak at 3450 cm^{-1}.

Bisacrylate monomer **2** and photoinitiator **3** were purchased from Shin-Nakamura Chemical and Merck, respectively.

Preparation of Cast Films and Polymerization. Bilayer-forming ammonium amphiphile **1** was dispersed in water by sonication (15 mM), and bisacrylate monomer **2** and photoinitiator **3** (2 mol % of the monomer) were added. The mixture was cast on fluorocarbon membrane filters (Sumitomo Electric Co., diameter 47 mm, pore size 0.1 μm) for 48 h at 25 °C and 60% relative humidity. Because of the low surface energy of the fluorocarbon membrane, the aqueous mixture did not penetrate into membrane pores. The resulting transparent film was subjected to polymerization by irradiating with a 500-W ultrahigh-pressure Hg lamp (Ushio Denki, Model UI-501C) for 90 s at room temperature and peeled off from the fluorocarbon membrane support. Extraction of the amphiphile component was carried out by dipping the bilayer/polymer composite film in fresh methanol repeatedly for 3 h. Complete removal of the amphiphile was confirmed by IR spectroscopy and elemental analysis. The single-component cast film (amphiphile alone) was prepared by casting an aqueous bilayer dispersion on a fluorocarbon membrane filter under the same conditions. A three-dimensionally cross-linked polymer was synthesized by photoirridation of a mixture of bisacrylate monomer **2** and photoinitiator **3** (2 mol % of the monomer), which was kept as a liquid film between quartz plates.

Measurements. The phase-transition behavior of cast films and aqueous bilayer dispersions was investigated by differential scanning calorimetry (Seiko Instruments, SSC-5000). Film samples (about 1 mg) or aqueous dispersions (ca. 45 mg of a 10 mM solution) were sealed in silver pans, and the scanning was repeated from 20 to 80 °C at a rate of 1 °C/min.

X-ray diffraction of cast films was obtained by the reflection method (2θ–θ scan) and by the transmission method (edge view) with a Rigaku Denki RAD-R-32 X-ray diffractometer. The X-ray beam was generated with a Cu anode, and the Cu Kα beam was taken out via a graphite monochromator (reflection method) and with a nickel filter (transmission method). The edge-view diffraction was obtained by directing the X-ray beam parallel to the film surface (thickness 100–150 μm) and by photographing by a plate camera.

XPS spectra were obtained on an ESCA 5300 X-ray photoelectron spectrometer (Perkin-Elmer), which was operated at 12 kV and 25 mA (300 W) with a Mg Kα X-ray source and at 5×10^{-9} Torr. Samples were cooled by liquid nitrogen. The survey spectrum in a range of 0–1000 eV was measured with a pass energy of 89.45 eV with a sampling step of 1.0 eV/step. The scan time was 1.0 min. In the narrow-region measurement (394–414 eV for the N_{1s} peak and 525–545 eV for the O_{1s} peak), the pass energy of 71.55 eV was used with a sampling step of 0.1 eV/step and a scan time of 1–2 min. The sample stage was tilted at different angles against the analyzer for angle-resolved measurements. Data analysis was carried out with an Apollo Domain 3500 computer.

Scanning electron microscopy (SEM; Hitachi S-900) was conducted for films fractured in liquid nitrogen and sputtered with Pt–Pd. Tensile strength and ultimate elongation of multilayered polymer films were measured with a tensile testing instrument (Orientec UCM-30) for a sample of 5 mm × 40 mm (thickness 30–40 μm for the two-dimensional polymer and 100–200 μm for the three-dimensional polymer, span 15 mm) at a tensile speed of 5 mm/min. In determination of swelling ratios, part of a polymer film was glued to a slide glass and its thickness and size (width and length) were measured by an optical microscope. Acetone was dropped on the film, and the size was measured after swelling had reached an equilibrium (10–30 s).

Results and Discussion

Preparation of Cast Films and Side-Chain Alignment. Glutamate-based double-chain ammonium amphiphiles form well-organized bilayer membranes because of their strong self-assembling property. They are also superior as components of regular cast films.[5] Cast films of amphiphile **1** are transparent and self-supporting when it is cast by itself as well as when it is cast together with a monomer component. A typical example of a composite cast film and its cross-sectional view are shown in Figure 1. A layered structure parallel to the film plane is clearly seen in the latter. The appearance and the layered cross-section of a cast film of **1** alone are virtually the same.

The component alignment in cast films can be estimated by measurement of the crystal to liquid crystal-phase transition of the bilayer by differential scanning calorimetry (DSC). A single-component cast film of **1** gives a sharp transition peak at 67 °C with ΔH of 82 kJ·mol^{-1}. An equimolar cast film of **1** and **2** gives a DSC peak at the same temperature with a ΔH of 89 kJ·mol^{-1}. These identical DSC peaks suggest that incorporation of the monomer does not affect the regular bilayer structure of the original cast film. The DSC peak after photopolymerization again appears at 67 °C (ΔH = 80 kJ·mol^{-1}) and indicates that the polymerization process does not interfere with the regular structure.

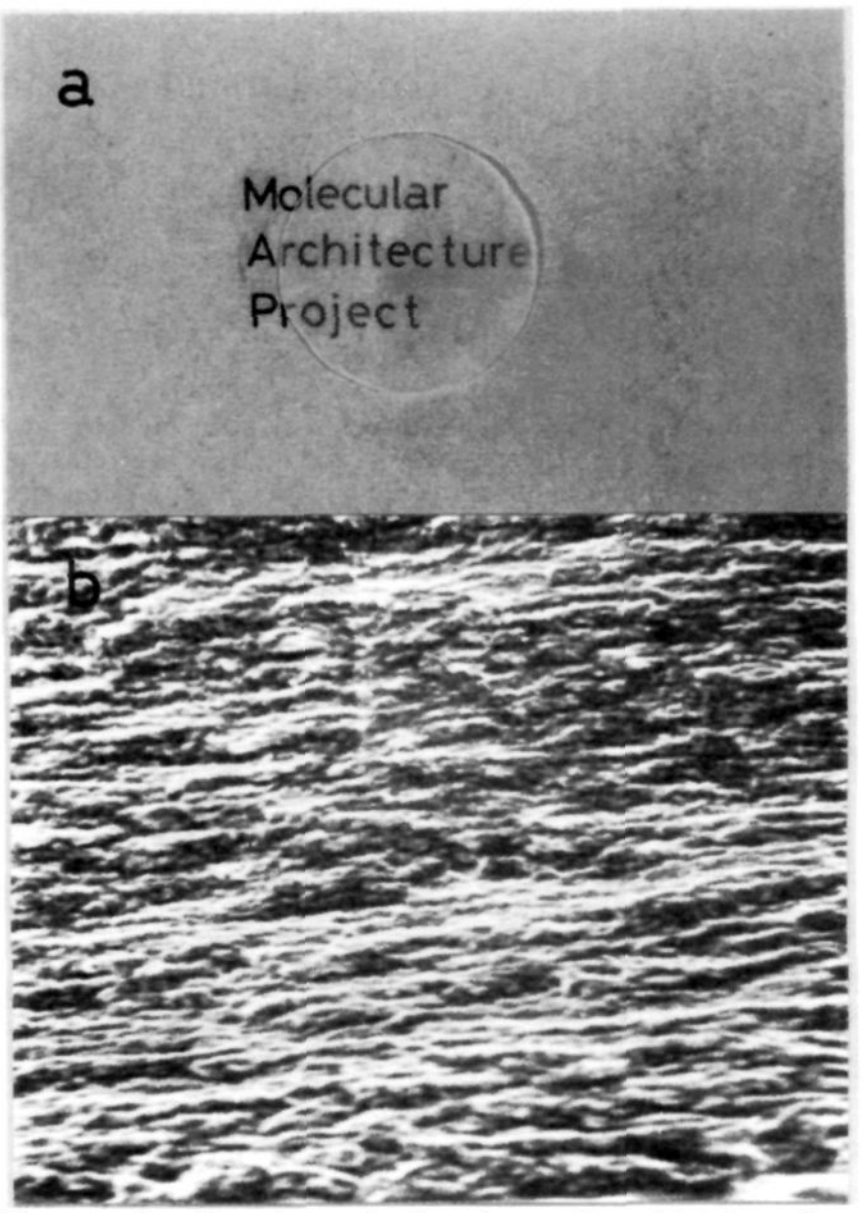

Figure 1. Cast film of an equimolar mixture of **1** and **2** (after polymerization): (a) photograph, diameter 30 mm; (b) cross-sectional view by scanning electron microscopy.

Two possibilities are conceivable for the insensitivity of the DSC characteristics to added monomer and polymer. The first is complete (macroscopic) segregation of the bilayer and monomer (or polymer) components in a cast film so that the original multibilayer structure is maintained without structural changes. The second possibility is a microscopic segregation in which monomer (or polymer) is accommodated in the interbilayer space without destroying the original bilayer assembly. The latter supposition was found to be valid from X-ray diffraction and XPS spectroscopy.

Regular Structure of Multibilayer Films. FIgure 2 compares reflection X-ray diffraction patterns of a single-component cast film and composite cast films. The single-component film gives a series of reflections, which correspond to a long spacing of 60 Å up to 10th order (Figure 2a). A composite film that contains 20 mol % (as monomer unit) of polymer shows two series of diffraction patterns, which are ascribed to long spacings of 60 and 74 Å (Figure 2b). The first series is lessened with increasing amounts of the polymer and totally disappears at more than 50 mol %. Diffraction data of an equimolar cast film are shown in Figure 2c in which diffractions up to 15th order due to a spacing of 74 Å are the only component. Further increases in the amount of polymer lower the diffraction intensity. A cast film of the 1:2 composition (amphiphile/polymer) still gives diffractions as-

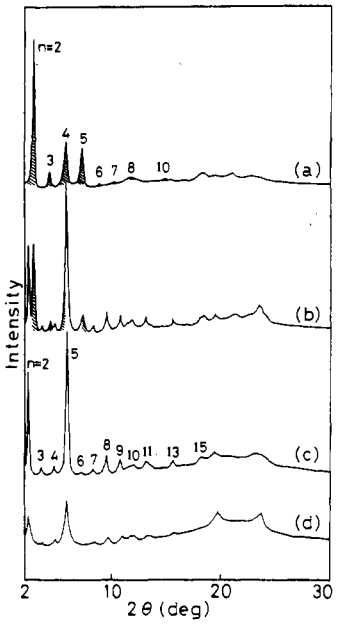

Figure 2. X-ray diffraction patterns of cast films obtained by the reflection method: (a) single-component cast film of **1**; (b) composite cast film of **1** and **2**, molar ratio 5:1 (after polymerization); (c) composite cast film of **1** and **2**, molar ratio 1:1 (afer polymerization); (d) composite cast film of **1** and **2**, molar ratio 1:2 (after polymerization). The order of diffraction is given. The shadowed peaks are ascribed to the spacing of the single-component structure (d = 60 Å).

cribable to a long spacing of 74 Å, but they are seen only up to 5th order and with much reduced intensities (Figure 2d).

Transmission X-ray diffraction patterns (edge view) are shown in Figure 3. The single-component film and the 1:1 component film give equatorial diffractions in the small-angle region, which correspond to the respective long spacings observed in the reflection diffraction and are consistent with the formation of multilayered structures. In addition, four diffractions corresponding to d = 3.5 Å are found, though diffuse, at the direction of 55° from the equator in Figure 3a, and two diffractions corresponding to d = 4.0 Å are seen on the meridian in Figure 3b. These diffractions in the wide-angle range are consistent with the component orientation such as discussed below. Diffractions due to a long spacing appear as rings in Figure 3c. This indicates that the extended regularity of the layer structure is lost when excess polymer is included.

The preceding diffraction data are interpreted as follows: Cast films of **1** can assume two stable assemblies with spacings of 60 and 74 Å. The multilayer structure of d = 60 Å is formed preferentially in the absence of the second component. Addition of monomer **2** (or its polymer) produces a new bilayer organization with an increased spacing. It is important to note that the change in the long spacing is a two-state process and is not a gradual transformation. This indicates that the composite cast film possesses an equally regular structure. When the amount of added monomer is not sufficient (20 mol %), two types of the bilayer organization coexist as separate phases. The second structure is stably formed when 50–100 mol % of the monomer is added. The multibilayer regularity deteriorates by further increases of the additive. It is clear that the additives are accommodated in the specific space that is created by a change in the bilayer organization. We can rule out nonspecific incorporation of additives into the interbilayer space. This conclusion is supported more fully by conducting a simulation of the bilayer structure by electron density matching as described below.

Simulation of Molecular Alignment in Bilayer by Electron Density Matching. Detailed X-ray structural studies were carried out for cast films of amphiphile **1** alone and an equimolar mixture of **1** and **2** (after polymerization). The structural simulation of synthetic bilayer membranes has been conducted by Okuyama and co-workers extensively.[23,24]

The integral reflection intensity (I_{obs}) that corresponds to the nth order diffraction was measured by the 2θ–θ scan and converted to the relative structure amplitude (F_{obs}) by

$$|F_{obs}(n)| = nI_{obs}(n)^{1/2} \quad (1)$$

which provides approximate Lorentz and polarization corrections.[25]

A molecular model for **1** within the bilayer organization was constructed as shown in Figure 4, in reference to the single-crystal X-ray analysis of simpler double-chain ammonium amphiphiles.[26,27] The alkyl groups were assumed to be all in the trans conformation. The molecular arrangement was assumed to be determined by four parameters: θ_1 (tilt angle of alkyl tail against the layer plane), θ_2 (dihedral angle between alkyl tail and spacer methylene), θ_3 (rotation of alkyl tail around the tail axis), and t (translation of ammonium nitrogen from the layer surface). The bromide counterion was assumed to be located at the identical translation, as has been found for other ammonium bilayers.[26]

The structural amplitude of nth order (F_{cal}) was calculated for each structure model that was generated by independent variations of the four structure parameters: θ_1 from 0 to 90° at an interval of 5°; θ_2 from −90 to +90° at every 5°; θ_3 from 0 to 360° at every 30°; and t from 0 to 4 Å at every 0.25 Å.

In the case of the polymer/bilayer composite film, the polymer molecule is most likely to stay in the spacer portion as discussed above. Therefore, its electron density was assumed to be in the Gaussian distribution with its peak top located at the midpoint of the spacer region along the film z axis.

The most plausible structures were selected as shown in Figure 5 for the smallest R factors: 0.11 and 0.22 for the single-component film and the 1:1 composite film, respectively.

$$R = \frac{\sum_n |F_{obs}(n)^2 - F_{cal}(n)^2|}{\sum_n F_{obs}(n)^2} \quad (2)$$

These R factors are sufficiently small to warrant the reliability of this simulation method.[28]

In the single-component cast film (Figure 5), the alkyl tail is tilted by 55° against the layer plane and the spacer methylene is tilted by an additional 25°. This difference in the tilt angles is required for packing adjustment of the double-chain tail and the single-chain spacer. In the composite film, the alkyl tails are placed normal to the layer plane and the tilt angle of the spacer methylene is 50°.

These tiltings of the alkyl chain inferred from the reflection X-ray intensity do not contradict the data of the transmission X-ray diffraction of Figure 3. Four-point-layer line scattering corresponding to d = 3.5 Å was observed at an angle of 55° from the equator for the single-component film, and a wide-angle scattering (d = 4.0 Å) was present for the composite film.

The void created in the spacer portion by the orientation change (Figure 5b) is actually filled with polymer chains (or monomer molecules). The Gaussian distribution is assumed for the electron density of the incorporated polymer. The assumption is not necessarily compatible with the simulation results in which a uniform molecular void is created in the spacer area. However, the value of the R factor (R = 0.22) is small enough to guarantee

(23) Harada, A.; Okuyama, K.; Kumano, A.; Kajiyama, T.; Takayanagi, M.; Kunitake, T. *Polym. J. (Tokyo)* **1986**, *18*, 281–286.
(24) Okuyama, K.; Ozawa, Y.; Kajiyama, T. *Nippon Kagaku Kaishi* **1987**, 2199–2204.
(25) Wilkins, M. H. F.; Blaurock, A. E.; Engelman, D. M. *Nature (London), New Biol.* **1971**, *230*, 72–76.
(26) Okuyama, K.; Soboi, Y.; Iijima, N.; Hirabayashi, K.; Kunitake, T.; Kajiyama, T. *Bull. Chem. Soc. Jpn.* **1988**, *61*, 1485–1490.
(27) Okuyama, K.; Iijima, N.; Hirabayashi, K.; Kunitake, T.; Kusunoki, M. *Bull. Chem. Soc. Jpn.* **1988**, *61*, 2337–2341.
(28) A systematic structure determination is being conducted in these laboratories for related double-chain ammonium amphiphiles. The present method gives satisfactory simulations in most cases: Okada, H. Manuscript in preparation.

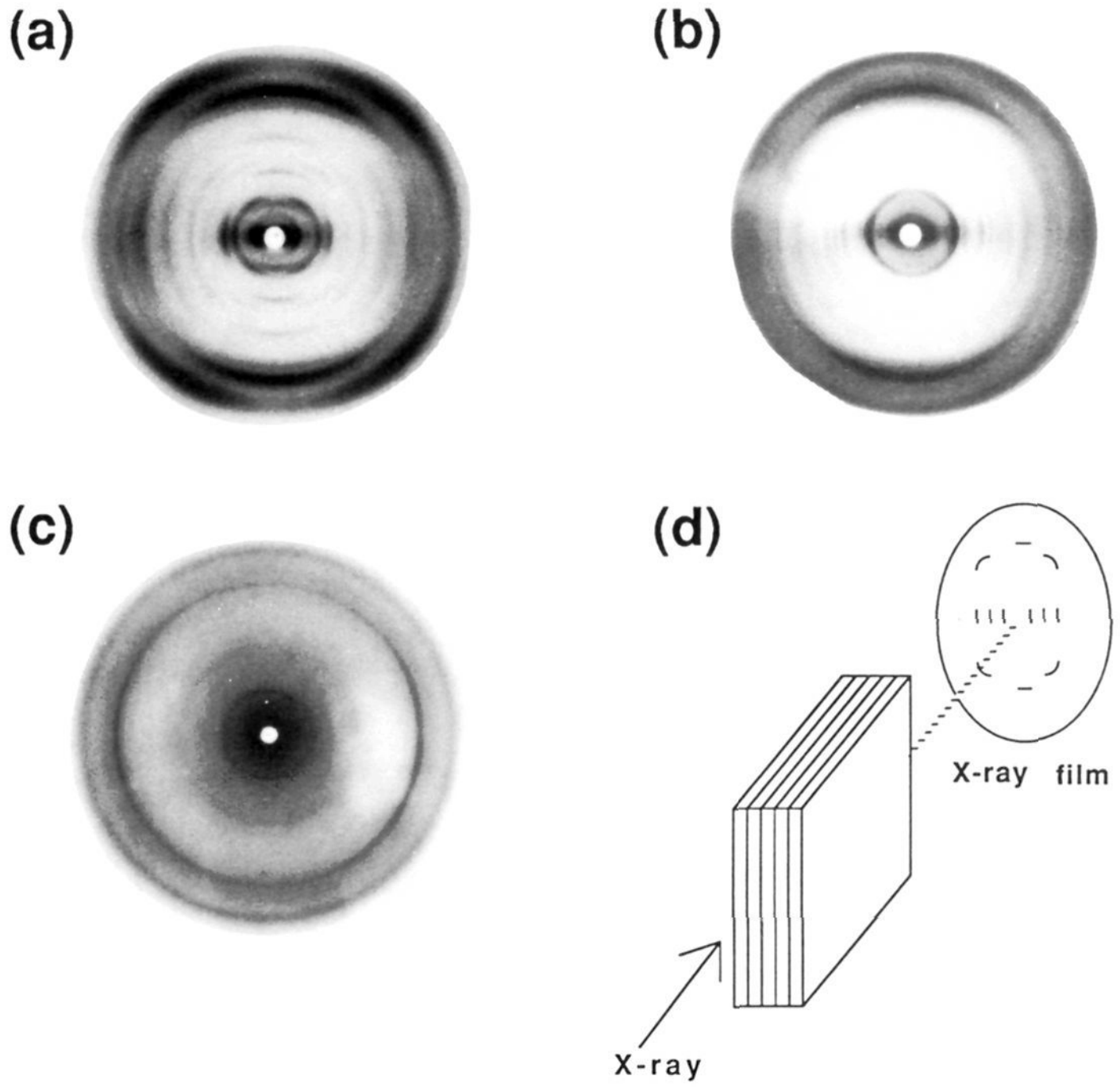

Figure 3. X-ray diffraction patterns of cast films obtained by the transmission method: (a) single-component cast film of **1**; (b) composite cast film of **1** and **2**, molar ratio 1:1 (after polymerization); (c) composite cast film of **1** and **2**, molar ratio 1:2 (after polymerization); (d) X-ray beam directed parallel to the film plane that is held vertically.

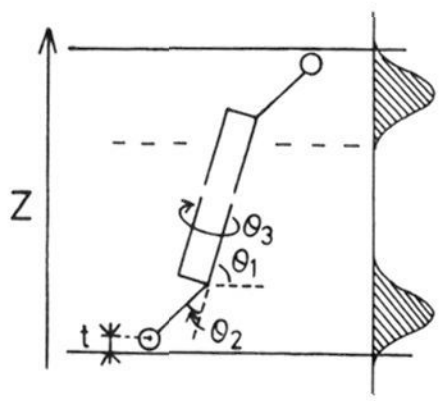

Figure 4. Parameters used for simulation of the molecular arrangement in cast films. See text for definitions of the parameters. The shadowed region indicates the Gaussian distribution of the electron density of the polymer component in composite films.

the usefulness of the simulation as a first approximation.

Determination of Molecular Composition by the XPS Technique. X-ray photoelectron spectroscopy has been applied to examination of surface concentration of a fluorocarbon component in cast multibilayer films[29-31] and to determination of the molecular orientation of azobenzene bilayers.[32,33] The above-mentioned simulation results are reinforced by depth analysis of the XPS data.

In XPS measurements, compositional information is obtainable from depth (d), which is 3 times larger than the mean free path (λ) of the photoelectron

$$d = 3\lambda \sin \theta \tag{3}$$

where θ is the takeoff angle.

The mean free path is determined by the kinetic energy of the photoelectron (E_k (eV)) and the bulk density (ρ) of the samples and is given for organic materials by[34]

$$\lambda \text{ (nm)} = \frac{49}{10^{-3}\rho E_k^{\,2}} + \frac{0.11 E_k^{\,1/2}}{10^{-3}\rho} \tag{4}$$

The bulk density of the cast films is 1.3 g cm^{-3}, and λ of the N_{1s} photoelectron is estimated from this equation to be 25 Å. This value is close to the value of 24 Å that is reported for the single crystal of an azobenzene amphiphile.[33] Thus, the compositional information is obtained for the depth of at most 70–80 Å, and sufficiently accurate results are expected if the two outermost molecular layers are taken into account in the following analysis.

(29) Higashi, N.; Kunitake, T.; Kajiyama, T. *Macromolecules* **1986**, *19*, 1362–1366.
(30) Takahara, A.; Higashi, N.; Kunitake, T.; Kajiyama, T. *Macromolecules* **1988**, *21*, 2443–2446.
(31) Takahara, A.; Morotomi, N.; Hiraoka, S.; Higashi, N.; Kunitake, T.; Kajiyama, T. *Macromolecules* **1989**, *22*, 617–622.
(32) Nakayama, Y.; Takahagi, T.; Soeda, F.; Ishitani, A.; Shimomura, M.; Kunitake, T. *J. Colloid Interface Sci.* **1988**, *122* (2), 464–474.
(33) Nakayama, Y.; Takahagi, T.; Soeda, F.; Ishitani, A.; Shimomura, M.; Okuyama, K.; Kunitake, T. *App. Surface Sci.* **1988**, *33*, *34*, 1307–1306.
(34) Roberts, R. E.; Allara, D. L.; Pryde, C. A.; Buchanan, D. N. E.; Hobbins, N. D. *Surf. Interface Anal.* **1980**, *2*, 5–10.

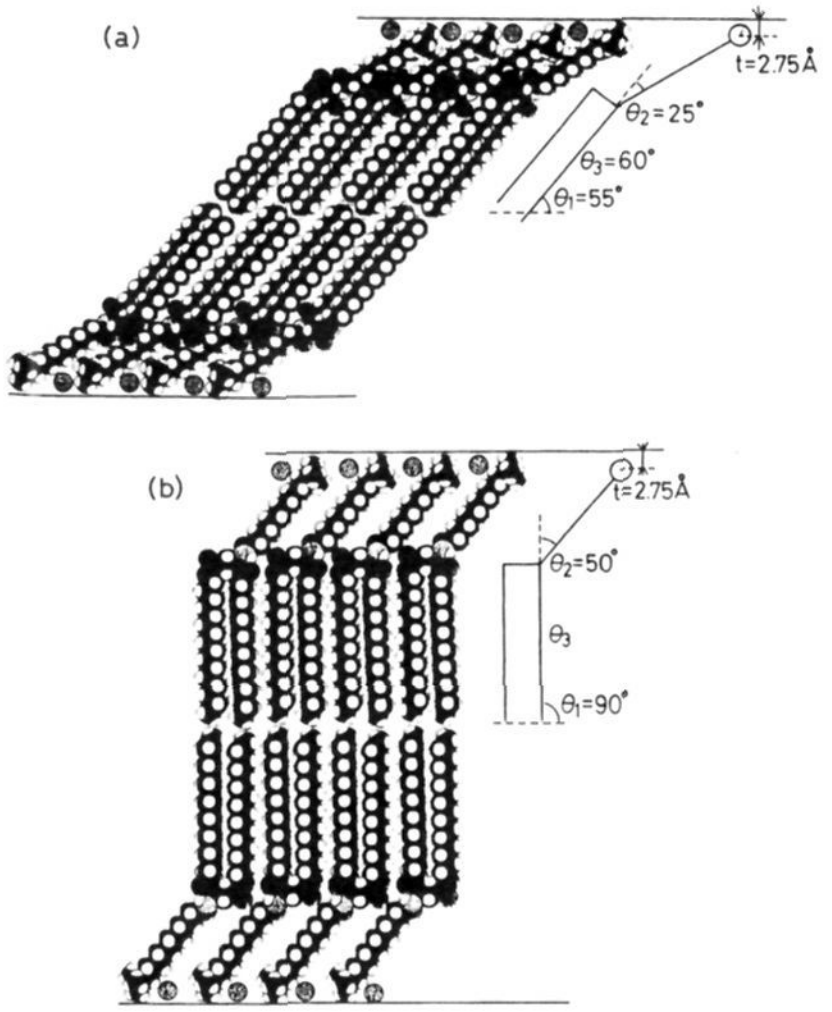

Figure 5. Most plausible molecular packings in cast films, as inferred from XRD data: (a) single-component cast film of **1**; (b) composite cast film of **1** and **2**, molar ratio 1:1. The θ_3 value cannot be determined in (b), as the alkyl tail is oriented parallel to the z axis.

The intensity of a photoelectron coming from depth d_x is given by

$$I = I_0 \exp[-dx/\lambda \sin \theta] \quad (5)$$

The relative intensity of N_{1s} peaks of ammonium and amide nitrogens at different takeoff angles is given by

$$I_{N(II)}/I_{N(I)} = \frac{\exp\left(-\frac{b}{\lambda \sin \theta}\right)\left\{1 + \exp\left(-\frac{c}{\lambda \sin \theta}\right)\right\}}{1 + \exp\left(-\frac{2b + c}{\lambda \sin \theta}\right)} \quad (6)$$

where b and c denote the depth difference between the amide nitrogen (N(I)) and the ammonium nitrogen (N(II)) of the outermost layer and that between the ammonium nitrogens of the first and second layers, respectively, as shown in Figure 6.

Figure 7 shows a wide-scan XPS spectrum of a single-component cast film. The N_{1s} region is composed of two peaks that are ascribable to the ammonium and amide nitrogens, as shown in the insert. The relative peak area of N(I)/N(II), which is estimated by curve fitting, increases with increasing probing depths (i.e., increasing takeoff angles), consistent with the presence of the ammonium nitrogen (N(I)) at a greater depth.

The relative intensity was theoretically estimated from eq 6, on the basis of the structural model of Figure 6. Depth parameters (a, b, and c) were determined from the packing structures of Figure 5. The calculated values are in satisfactory agreement with the experimentally observed data in both cases: Figure 8a. This is a strong support for the multilayer organizations inferred from simulations of the X-ray diffraction data.

The relative intensity of the O_{1s} peak and the amide N_{1s} peak is plotted against takeoff angles in Figure 8b. A slightly decreasing trend is found for the single-component cast film because the amide nitrogen atom is located deeper than the ester oxygen atom. The O_{1s} peak is stronger at all θ ranges in the case of the composite film due to the presence of the oxygen-rich polymer. In particular, the relative intensity ($I_O/I_{N(II)}$) of this film is much enhanced at

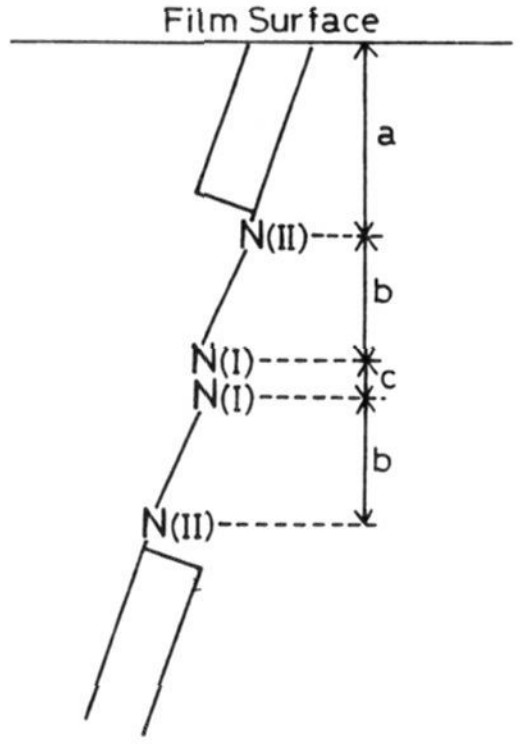

	Single-component cast film	Composite cast film
Depth of N(II) from surface, a	19.7 Å	24.0Å
Depth difference between N(I) and N(II), b	8.0Å	10.3Å
Distance between opposing N(I)'s, c	5.5Å	5.5Å

Figure 6. Distances (depths) of the ammonium and amide nitrogens from the film surface. These values are estimated from the packing data of Figure 5.

the largest takeoff angle. This result is consistent with the supposition that the polymer molecule is localized deep in the spacer area. Theoretical estimation of the relative intensity was not easy in this instance because the mean free path of the O_{1s} electron (22 Å) is different from that of the N_{1s} electron and the atomically exact disposition of the polymer molecule is not known.

Recovery of the Multilayered Polymer Network. The equimolar composite film was subsequently immersed in methanol at room temperature in order to wash out the bilayer matrix. The film swelled to a certain extent. Methanol was replaced five to six times in 3 h, and the remaining film (two-dimensional polymer) was dried. This film was flexible and self-supporting as shown in Figure 9a, and its thickness and surface area were 50% and 80%, respectively, of the original sizes. A sufficiently dried film (5 h, in vacuo) gave the following elemental analyses: C, 53.64; H, 8.22; N, 0. These values are in good agreement with those (C, 53.94; H, 8.22) of a bulk-polymerized film (three-dimensional polymer, the bilayer component not added), indicating complete removal of the matrix bilayer. No significant differences were found between FT-IR spectra of these polymers. The amount of the residual vinyl unit was not detectable by FT-IR spectroscopy.

Raman scattering spectra of Figure 10 indicate almost complete consumption of the vinyl group in the two- and three-dimensional polymers. The residual vinyl group appears to be less than 5% in either case, which indicates occurrence of extensive cross-linking.

A greatest structural difference of the extracted cast film relative to the three-dimensional polymer is seen in an SEM photograph of its cross-section. Figure 9b clearly shows that wavy-layer structures are formed parallel to the film surface. This fine structure is not at all found in the cross-section of the three-dimensional polymer film. The layer thickness appears to be 20–100 nm: This unit thickness is much larger than would be expected from the combined spacer region of a regular composite structure. The SEM resolution is limited, and several unit layers may be stuck together during the preparation of the SEM

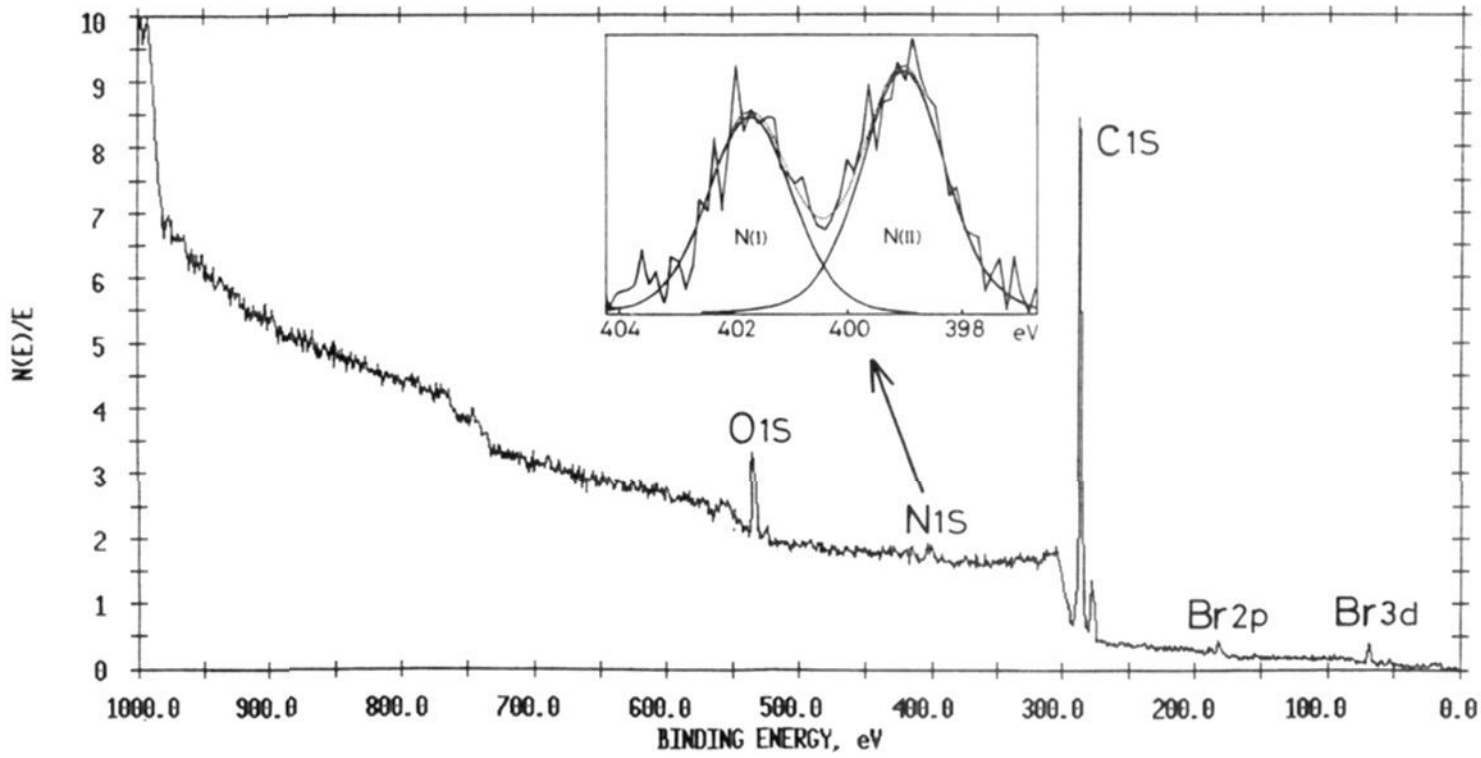

Figure 7. Wide-scan XPS spectrum of a single-component cast film of **1** measured at a takeoff angle of 45°. The inset shows deconvolution of the N_{1s} peak.

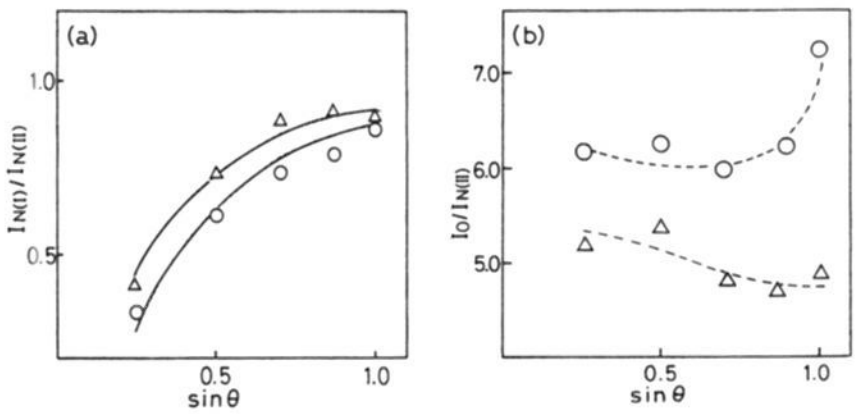

Figure 8. Depth profile of XPS peak ratios of cast films: (a) peak area ratio of the ammonium and amide nitrogens (N(I) and N(II)) for the single-component cast film (△) and for the composite cast film (○), solid lines calculated from the structure models of Figure 6; (b) variation of the area ratio of the O_{1s} and N_{1s} (amide) peaks with takeoff angle θ.

Table I. Mechanical and Swelling Properties of Two- and Three-Dimensional Polymers

polymer	tensile strength (kg/mm²)	ultimate elongation (%)	swelling ratio[a] (%)	
			lateral	perpendicular
2D	0.60	48	15	69
3D	0.20	11	13	12

[a] Measurement in acetone.

specimen. The polymer is rubbery at room temperature. This may also cause the loss of the original fine structure.

Physical Properties of the Two-Dimensional Polymer Network. Swelling of the two- and three-dimensional polymer films was measured in acetone at room temperature, and the result was summarized in Table I. The swelling ratios of the three-dimensional polymer film are essentially the same in the lateral as well as perpendicular directions. In contrast, the perpendicular swelling was ca. 5 times greater than the lateral swelling in the case of the two-dimensional polymer film. This is a strong indication of the presence of anisotropic cross-linking. The solvent would be readily accommodated in between the two-dimensional polymer networks.

The anisotropic structural characteristics are also evident in some mechanical properties. As included in Table I, the tensile strength of the two-dimensional film is 3 times greater than that of the three-dimensional film and the ultimate elongation of the former is also ca. 5 times greater. It is known that formation of microgels leads to nonuniform cross-linking in three-dimensional gels,[35,36] which results in limited strength and elongation. In

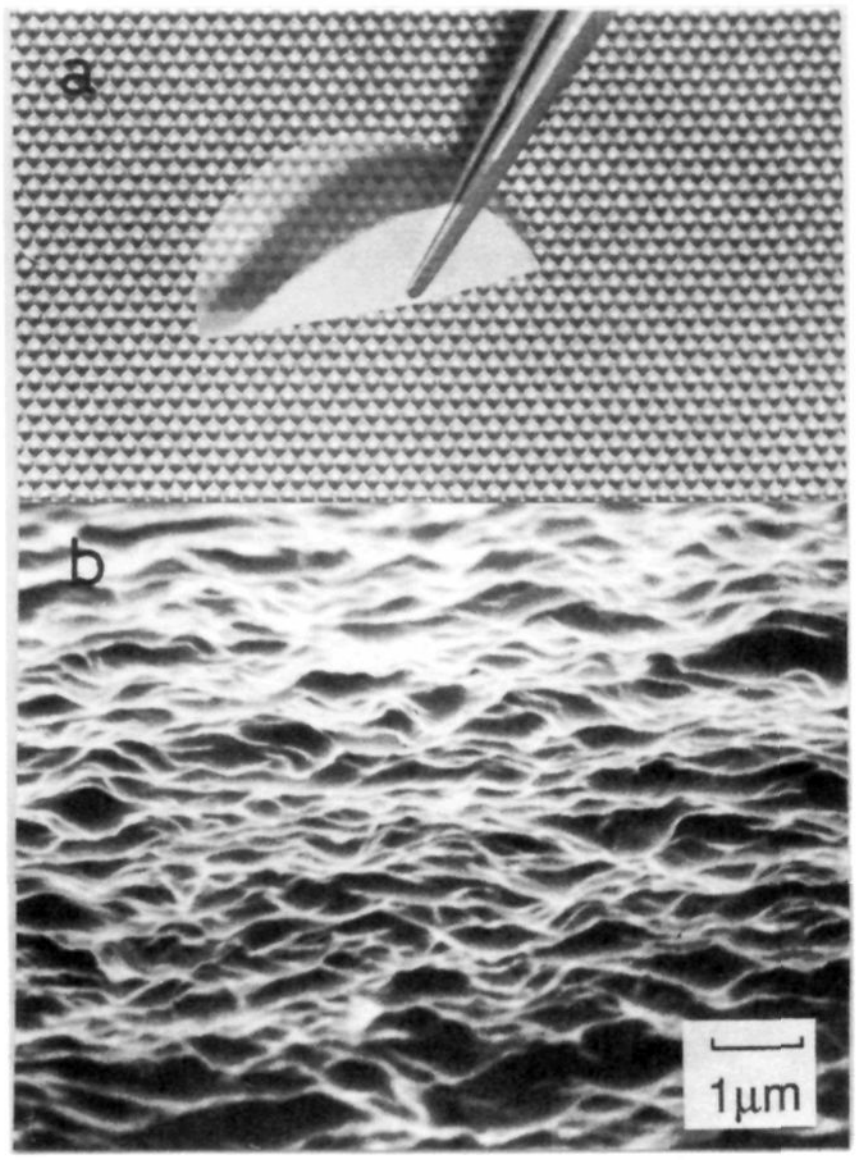

Figure 9. Multilayered film of two-dimensional polymer network: (a) photograph, diameter 25 mm; (b) cross-sectional view by scanning electron microscopy.

contrast, the monomer molecules in an equimolar composite film are uniformly distributed with thicknesses of several tens of angstroms and cross-linking is expected to extend uniformly in the two-dimensional space. Localization of applied stress should be avoided due to slipping of stacked two-dimensional networks. These structural characteristics are conceivably related to improved

(35) Horie, K.; Otagawa, A.; Muraoka, M.; Mita, I. *J. Polym. Sci., Polym. Chem. Ed.* **1975**, *13*, 445–454.
(36) Galina, H.; Dusek, K.; Tuzar, Z.; Bohdanecky, M.; Stokr, J. *Eur. Polym. J.* **1980**, *16*, 1043–1046.

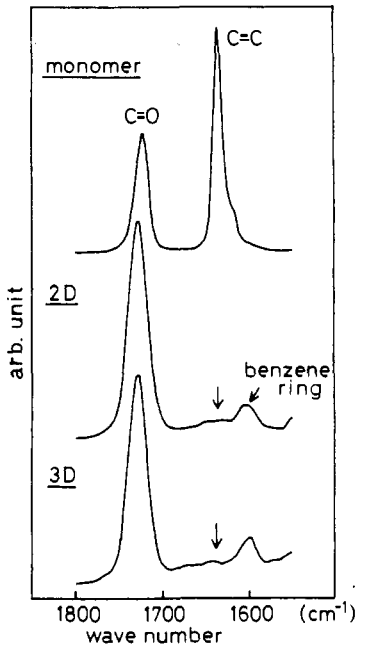

Figure 10. Raman scattering spectra of monomer **2**, a multilayered polymer film (two-dimensional), and a bulk-polymerized polymer film (three-dimensional).

mechanical properties of the two-dimensional film.

Concluding Remarks

It is established that cast multibilayer films are superior molecular templates for preparation of two-dimensional polymer networks. Figure 11 schematically represents the procedure to obtain two-dimensional molecular networks. Composite cast films are prepared in such a way as to maintain regular, layered structures. Template amphiphile is removed upon immobilization of the guest component. The preceding experimental evidence, expecially X-ray diffraction and XPS data, proves that highly regular composite films are formed. It is important that a regular structure is formed at specific molar ratios of template bilayer and guest polymer. This regularity is crucial in order that the network formation be confined in the two-dimensional interbilayer space of the film. Definitive evidence was not obtained here for the network formation with molecular thickness. Unfortunately, the molecular resolution is not attained by the present SEM technique. The rubbery nature of the polymer also makes it difficult to observe extended two-dimensional structures. In fact, we could observe formation of ultrathin (ca. 20-Å thickness) layers from a more rigid siloxane network by the same technique.[22]

Preparation of two-dimensional molecular networks has been investigated by other workers at interfaces and at interlayer spaces, as described in the Introduction. The most notable advantage of the present methodology is its experimental flexibility. Synthetic

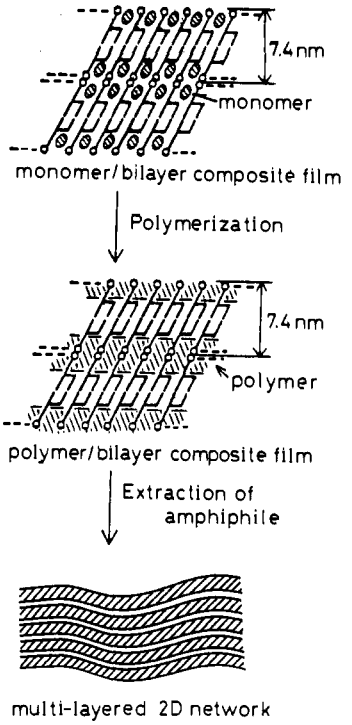

Figure 11. Schematic illustration of template synthesis of a multilayered two-dimensional polymer network.

bilayer membranes are self-assembling molecular systems. Therefore, incorporation of guest molecules into interbilayer space of cast films does not destroy the original bilayer assemblage. This unique property allows the use of widely variable guest molecules for the subsequent immobilization. The large structural variety of synthetic bilayer membranes further enhances the flexibility of the system.

It is interesting to compare the present methodology with the Langmuir–Blodgett (LB) technique. The two-dimensional organization of cast multibilayer films can be transplanted in other molecular systems that would not form the two-dimensional ordering in their own right. The requirements for the guest molecule are minimal: uniform incorporation into the interbilayer space and the subsequent successful immobilization. The advantage of the LB technique is preparation of very thin molecular layers and separate control of each layer. However, component molecules are limited in that they have to produce stable monolayers. Much more variable two-dimensionally organized materials would be synthesized by the present technique.

Registry No. 1, 107066-31-9; **1** diester, 59274-90-7; **1** amide, 131237-11-1; **2** (homopolymer), 131237-16-6; **3**, 106797-53-9; $H(CH_2)_{10}OH$, 36653-82-4; $Br(CH_2)_{10}COCl$, 15949-84-5; trimethylamine, 75-50-3; L-glutamic acid, 56-86-0.